Experimental Evidence of Icosahedral and Decahedral Packing in One-Dimensional Nanostructures

J. Jesús Velázquez-Salazar,[†] Rodrigo Esparza,[†] Sergio Javier Mejía-Rosales,[§] Rubén Estrada-Salas,[†] Arturo Ponce,[†] Francis Leonard Deepak,[†,‡] Carlos Castro-Guerrero,[†] and Miguel José-Yacamán[†,*]

[†]Department of Physics and Astronomy, The University of Texas at San Antonio, One UTSA Circle, San Antonio, Texas 78249, United States, [‡]International Iberian Nanotechnology Laboratory, Avenida Mestre Jose Veiga, Braga 4715, Portugal, and [§]Center for Innovation and Research in Engineering and Technology, and CICFIM—Facultad de Ciencias Físico-Matemáticas, Universidad Autónoma de Nuevo León, San Nicolás de los Garza, NL 66450, México

ABSTRACT The packing of spheres is a subject that has drawn the attention of mathematicians and philosophers for centuries and that currently attracts the interest of the scientific community in several fields. At the nanoscale, the packing of atoms affects the chemical and structural properties of the material and, hence, its potential applications. This report describes the experimental formation of 5-fold nanostructures by the packing of interpenetrated icosahedral and decahedral units. These nanowires, formed by the reaction of a mixture of metal salts (Au and Ag) in the presence of oleylamine, are obtained when the chemical composition is specifically Ag/Au = 3:1. The experimental images of the icosahedral nanowires have a high likelihood with simulated electron micrographs of structures formed by two or three Boerdijk—Coxeter—Bernal helices roped on a single structure, whereas for the decahedral wires, simulations using a model of adjacent decahedra match the experimental structures. To our knowledge, this is the first report of the synthesis of nanowires formed by the packing of structures with 5-fold symmetry. These icosahedral nanowire structures are similar to those of quasicrystals, which can only be formed if at least two atomic species are present and in which icosahedral and decahedral packing has been found for bulk crystals.

KEYWORDS: Boerdijk—Coxeter—Bernal helix · nanowires · icosahedra · decahedra · aberration-corrected electron microscopy

A fascinating problem in material sciences is that concerning the packing of spheres to produce a dense structure. Although this problem has been studied probably since the ancient world, the first scientific analyses came from the Kepler conjecture: how to stack cannon balls of equal size with the highest packing density. The solution is the ABC fcc stacking with a packing density of 0.7405. The packing of spheres has important applications in the structure of liquids, crystals, glasses, and biological systems among others, for which the reader is referred to the excellent review by Torquato and Stilinger.[1]

Back in 1952, Boerdijk[2] described a particular type of packing in which if spheres are forming a tetrahedra, then it is possible to pack regular tetrahedra with a helical structure. If we start with a reference point in the center of the first tetrahedron, then a second tetrahedron can be stacked in such a way that one of its faces in the original position coincides with another of its faces on the second position. We can stack tetrahedra along a screw axis by rotating each tetrahedron by an angle of 131° 49′ with respect to its immediate neighbor. The resulting structure is known as the Boerdijk—Coxeter helix, after the work of Coxeter, who described similar structures when studying five-dimensional polytopes.[3] This is the first known structure that establishes a direct relation between helices and close packing; an atomistic representation of this structure is shown in Figure 1.

Tetrahedra cannot fill Euclidean space regularly; however, in a positively curved space they make a regular polytope {335} in which each object is immersed in an icosahedral environment.[4] In Euclidian space structures made with this type of helicoidal chains can be accommodated only by the introduction of topological defects. River and Sadoc[4] have used the polytype {335} to describe biological helices such as the alpha-helix and the collagen helix, and the Boerdijk—Coxeter[3] spiral was used by Lord and Ranganathan[5] to describe the γ-Brass structure. This structure was popularized by Bernal in his description of the structure of liquids,[6] and here we suggest that the structure should be called Boerdijk—Coxeter—Bernal helix, or BCB, for short.

Recently, Torquato and Yiao[7,8] studied the packing of platonic and Archimedean solids. A very significant result is that this packing produces a much larger density (ø), which can eventually be as large as 0.95. The fact that the tetrahedron has a large aspheric and lack of central symmetry contributes

* Address correspondence to miguel.yacaman@utsa.edu.

Received for review April 4, 2011 and accepted July 26, 2011.

Published online July 26, 2011
10.1021/nn202495r

© 2011 American Chemical Society

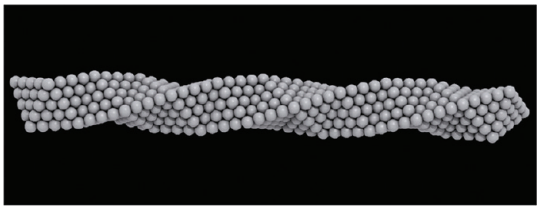

Figure 1. Boerdijk–Coxeter–Bernal helix. The BCB structure is made of tetrahedral sections sharing faces and following a straight line.

to increase the packing of the tetrahedron, which leads to a pentagon bipyramid or a decahedron. It is well known that tetrahedra do not fill the Euclidean space. For instance, when five tetrahedra are stacked in a cyclic way (twinning), the resulting decahedra is left with a 7° 36′ internal gap. Twelve interpenetrating decagonal pyramids result in an icosahedron. In a recent work, Haji-Akdari *et al.*[9] have shown that packing of tetrahedra will result in quasicrystalline phases; in particular they report the forming of a decagonal quasicrystal. The packing of icosahedra was discussed theoretically by Bilalbejovic,[10] using Monte Carlo calculations to study the aggregation, and it was found that linear, nanowire-like structures are produced. However, no mention is made of any connection with the BCB helices.

On the experimental side most of the work has been related to model systems, pioneered by Bernal about 50 years ago.[6] More recently, an experimental helical structure of gold nanowires was reported by Kondo and Takayanagi.[11] These authors synthesized helical multishell gold nanowires in an ultrahigh vacuum; the thinnest wire they were able to make was 0.6 nm in diameter, corresponding to a two-shell nanowire. This kind of structures consists of a tube formed by atoms coiled around the nanowire axis. According to the theoretical models of these structures, the axis has a central line of atoms (much like a coaxial cable).[12,13]

On the synthesis side an important advance has been achieved in growing nanowires. Halder and N. Ravishankar[14] introduced a synthesis method based on the reaction between chloroauric acid and oleylamine in a toluene medium. The problem with their method is that the growth is much uncontrolled, and nanowires of all sizes are produced along with nanoparticles.

An important improvement was made by Wang and co-workers,[15] who reported the growth of thin gold nanowires by the reduction of $HAuCl_4$ in oleic acid and oleylamine, which serves both as a reducing agent and a stabilizer. In this case the crystal structure corresponded to a standard fcc bulk, as confirmed by X-ray diffraction and high-resolution electron microscopy.

A similar method for the growth of very thin nanowires of gold was used by Hou *et al.*,[16] Lu et al.,[17] and Li *et al.*[18] However, they added Ag to further promote linear growth by reducing a complex of AuCl and

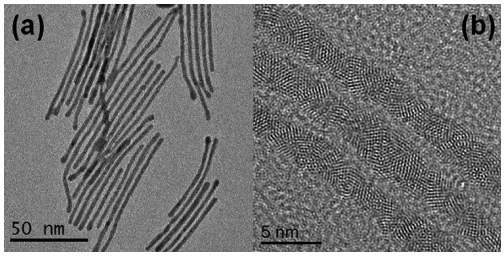

Figure 2. (a) TEM image and (b) HRTEM bright-field image of the icosahedral nanowires of Ag/Au.

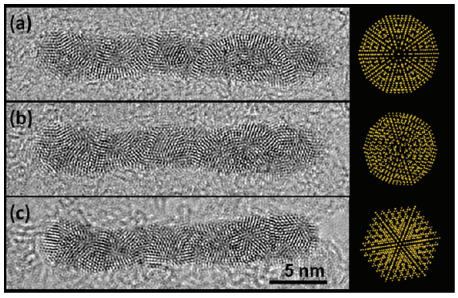

Figure 3. Tilting sequence of HRTEM images of the Ag/Au nanowires with the icosahedral structure: (a) angle of initial reference; (b) five-degree longitudinal rotation; and 10-degree longitudinal rotation.

oleylamine. It has been established that because of van der Waals interactions between the ends of the linear oleylamine chains, which are bonded to the Au^{I} ions, the growth of the Au metal takes place in a one-dimensional fashion. The resulting nanowires are fcc in structure and tend to be several micrometers long.

A particularly interesting case is that of the bimetallic nanowires. Krichevski *et al.*[19] have grown Ag/Au nanowires in a 1:1 proportion. These authors do not report any deep structural characterization of the nanowires. However, it must be assumed that they are fcc (this point will be discussed later). More recently Hong *et al.*[20] reported the growth of bimetallic Au/Ag nanowires in a proportion Au/Ag = 2:1. In this case a full electron microscope characterization showed that the nanowires are fcc.

Here, we report for the first time the experimental synthesis of gold nanowires that are formed by packing of icosahedra or decahedra along the growth axis. These structures were prepared using wet chemistry synthesis following methods proposed in the literature.[14–18] Specifically, we used oleylamine in a mixture with AuCl, and following the method of the Xia group,[18] we added silver salt to the solution and then reduced the salt under well-controlled conditions. The main differences with respect to previous work were that the reduction was made at a higher temperature and that the amount of silver was in a mole ratio of 2:1 Au/Ag, compared to the 200:1 ratio used by Li *et al.*[18]

RESULTS

The synthesis resulted in a sample containing 85% nanowires. The samples were examined by high-resolution

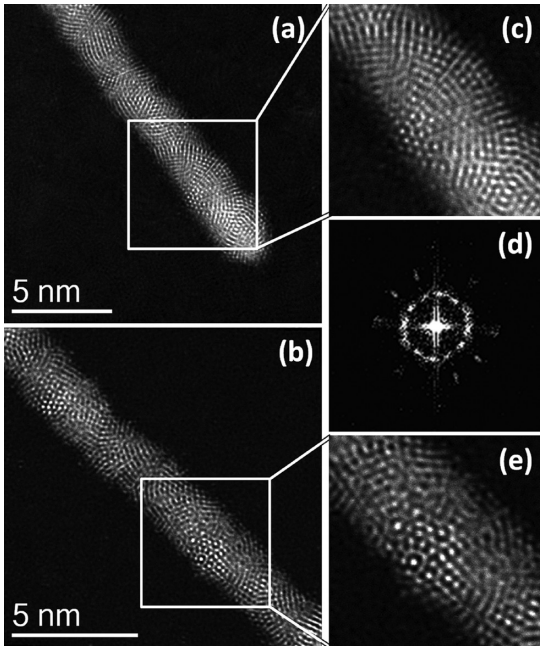

Figure 4. (a, b) Aberration-corrected STEM-HAADF images of the Ag/Au nanowires with the helical icosahedral structure in different orientations. The images (c) and (e) are the corresponding high-magnification areas of the icosahedral packing. The image (d) shows the FFT obtained along the axis of the nanowire of (a) showing the 5-fold symmetry.

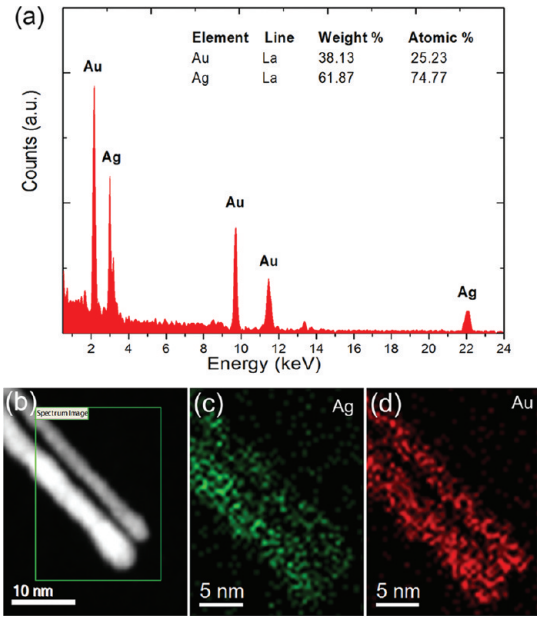

Figure 5. EDS analysis of two Ag/Au nanowires showing (a) the spectrum and the inset showing the concentration of Ag and Au, (b) the STEM image of two nanowires, (c) maps of the Ag L line, and (d) the Au L line.

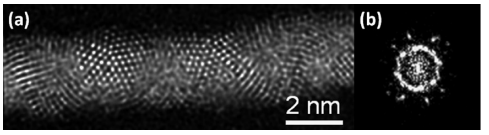

Figure 6. (a) Aberration-corrected STEM-HAADF image of the helical array of decahedral nanowire; (b) FFT obtained along the axis of the nanowire.

electron microscopy (HRTEM). A typical image is shown in Figure 2a. The atomic resolution contrast clearly shows a crystal stacking that is not a simple fcc (Figure 2b). The images reveal that the nanowire is made of individual icosahedral units, which are stacked along the growth axis. The HRTEM images of icosahedral particles have been well documented in the literature and can be easily recognized (see for instance the work of Marks[21] or Ascencio *et al.*[22]). Perhaps the clearest feature is that starting from the characteristic 5-fold symmetry axis, and upon rotation, 3-fold and 2-fold axes can be obtained. So in order to confirm the structure, we performed a tilting series of nanowires in the HRTEM mode. The tilting sequence of images is shown in Figure 3. We also show the model of an icosahedral particle along the image as an aid to recognize the 5-fold symmetry. It is clear that the nanowire contains elements of icosahedral symmetry.

To confirm this observation, we carried out a detailed analysis of the nanowires in an aberration-corrected STEM using the high-angle annular dark-field scanning transmission electron microscopy (HAADF-STEM) technique. In this technique the contrast is strongly influenced by the atomic number and mass, and the images do not change significantly with variations in defocus,[23] which makes the analysis straightforward. On carrying out high-resolution STEM-HAADF imaging of the nanowires, we observe clearly regions in 5-fold symmetry, as shown in Figure 4. In this figure we show the HAADF-STEM images of two nanowires with atomic resolution (Figure 4a and b). Following the structures along the growth axis under high magnification (Figure 4c and e) it was not difficult to realize that the structures correspond to arrays of interpenetrated icosahedra. The two images correspond to two slightly different orientations. We also obtained the Fast Fourier Transform (FFT) along the growth axis of the nanowire of Figure 4a; the result shown in Figure 4d confirms 5-fold symmetry.

We performed X-ray analysis in the STEM, and a detailed compositional analysis of the spirals was obtained. The result is shown in Figure 5. In the figure we show the EDS spectrum and the mapping of Au and Ag. The results clearly indicate that there is an excess of silver on the spirals. In some cases we measured a majority of silver on the structure with a molar composition of Ag/Au = 3:1. It is also clear that the two elements are homogeneously distributed along the nanowire, suggesting an alloy. We analyzed more than 10 nanowires, and the atomic concentration was the same. We consider this very remarkable and in contrast with the authors' experience in bimetallic particles, in which the concentration of the two metals seems to vary from particle to particle despite the initial

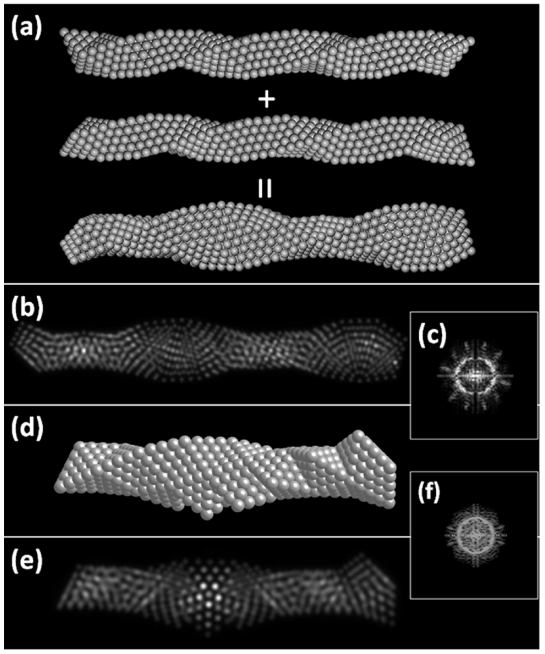

Figure 7. (a) Construction of a helical nanowire by the entanglement of Boerdijk–Coxeter–Bernal helices. Two BCB structures are shown, before and after the entanglement. (b) Simulated STEM image of the model. (c) Simulated diffraction pattern of the structure. (d) Model of the decahedral nanowire structure. (e) Simulated image of the decahedral nanowire structure. (f) Simulated diffraction pattern of the decahedral nanowire structure.

concentration during the reaction. In the latter case we can only speak of an average concentration, the composition of every particle being different. In the present case the atomic ratio is the same in each structure, which is quite remarkable.

In addition to the nanowires with icosahedral stacking we have also observed another type of nanowire with a 5-fold symmetry, as shown in Figure 6a. In this case the 5-fold symmetry corresponds to that of a decahedron, as this type of contrast cannot be explained as resulting from icosahedra stacking. The FFT along a nanowire with decahedral symmetry confirms the helical structure, as shown in Figure 6b.

Decahedral nanowires coexist with the icosahedral ones and with fcc nanowires. In a typical sample prepared under the conditions described in this paper 70% of the nanowires will be icosahedral, 20% decahedral, and 10% fcc or polycrystalline.

Structural Model of the Nanowires. In order to understand the structure of the nanowires reported in the present work, it is important to make some considerations. First, the nanowires found in this work are different from the helical nanowires found experimentally by Kondo and Takayanagi[11] and then studied extensively by the Ugarte group.[24–26] Those helical structures are only two or three atomic layers and are only produced by strain. Sanchez-Portal *et al.*[27] were the first ones to predict those structures theoretically using first-principle simulations under tensile loading.

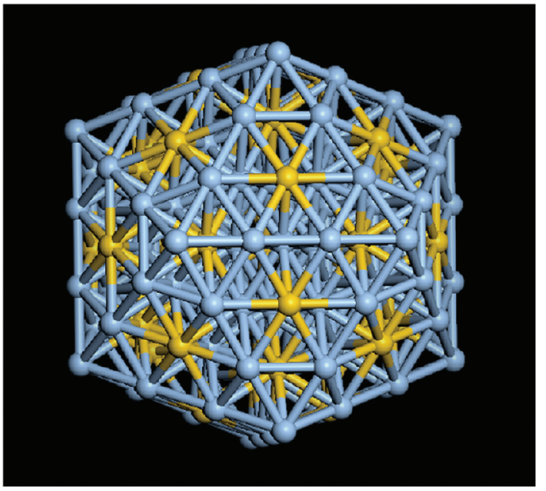

Figure 8. 147-atom icosahedron with an Ag/Au = 3:1 elemental ratio. Each tetrahedron in the structure is made of 3 silver atoms and 1 gold atom.

They conclude that these structures will break and cannot be isolated, as shown by Park and Zimermann.[28] The helical structure has a large amount of deformation and the atoms have a low coordination number, and because of that and the continuous stress, the atoms cannot create highly packed reoriented surface facets.

The nanowires reported in this work can have a thickness up to 20–30 atomic layers; they are also very long (as much as 50 nm). They are not the result of strain. Therefore a new structure has to be considered. A first simple model is that the growth under the conditions described in this paper induces icosahedral and decahedral particles. The nanowires would be then the result of coalescence of icosahedral and decahedral particles. A model of the nanowire formed by joining the decahedra by their (111) facets certainly induces a spiral but does not explain the observed contrast. A model is shown in the Supporting Information (Figure S2). In particular the "fan" type of contrast so conspicuous in the images is not reproduced by this model.

A third model can be obtained by winding together like a rope two or more B–C–B spirals and then relaxing the structure. A model is shown in Figure 7a for the case of two spirals. The model that results is that of interpenetrating icosahedra, which corresponds to truly icosahedral growth. This model reproduces remarkably well the contrast and the FFT as shown in Figure 7b,c. As can be seen, the "fan-like" 180° contrast is fully reproduced. A similar model can be obtained for the decahedral packing, which is formed by the interpenetration of decahedral spirals shown in Figure 7d,e.

In order to understand the role of the atomic composition of silver–gold, we have performed energetic calculations on an icosahedral structure of 147 atoms with an Ag/Au ratio of 3:1. At this particular ratio of elements, it is possible to distribute both atomic species in such a way that all the tetrahedra forming

the icosahedron are constituted by one atom of gold and three atoms of silver. The resulting structure is shown in Figure 8. We performed a molecular dynamics simulation run on this structure, using the many-body Sutton–Chen potential to describe the atomic interactions. Following the conditions of the experimental measurements, the simulation was performed at 300 K, and the average configurational energy was measured and compared against the energies of two icosahedral particles of the same size and composition, but with a random elemental distribution in one particle and an $Au_{core} - Ag_{shell}$ distribution on the other. We found that the configurational energy is very similar in the three cases, around 2.8 eV per atom. These results indicate that at the particular Ag/Au ratio of 3:1 the uniformly distributed structure is energetically as possible as two of the most likely alternatives. The comparison of these results against other relative concentrations will improve the understanding of the predominance of this ratio in the experimental structures, and future work of this group this will be devoted to this issue.

DISCUSSION

It appears that the addition of silver in the concentration Ag/Au increases the stability of icosahedral and decahedral structures. During most of the solution phase synthesis an equilibrium condition is not established. Under these conditions, structures that are not the equilibrium shape (Wulff polyhedron) such as icosahedra are formed.[29] In these structures, defects such as twins and steps lower the total free energy. In the case of Au, it is possible to grow very large particles with icosahedral or decahedral structure since new types of defects appear as size increases.[30] The main reason is that (111) facets are preferred in gold. The case of silver (100) is also prominent, and in most cases the particles tend to be pyramids or triangles. In rare cases icosahedra or decahedra are formed. However, in a recent paper Cerbelaud *et al.*[31] using DFT full calculations demonstrated that in Ag/Au alloy nanoparticles the icosahedral structure can be generated for ratios such as Ag/Au = 5.3, Ag/Au = 2.8, and Ag/Au = 2.16, which is in agreement with our results. It has been reported by Huo *et al.*[16] that during the growth of nanoparticles and nanowires using a mixture of AuCl and oleylamine a mesostructure is formed and the gold ions are assembled within the oleylamine bilayers. This mesostructure serves as a template for the growth in one dimension, resulting in nanowires. A similar mechanism was proposed by Lu *et al.*[17] When only Au was used, fcc nanowires are formed. However in our case when AgCl is added to the solution, the mesostructure will be formed but containing Au^+ and Ag^+ ions. In some regions, isolated units containing Au and Ag will be formed between them, separated by the oleylamine bilayer. When the reduction takes place, the atoms will tend to form icosahedra. Then when new atoms arrive, the icosahedral growth will continue in one direction templated by the oleylamine bilayer. The situation is similar to the formation of quasicrystals, which are produced only when at least two metals are present.[32]

Properties of Icosahedral Nanowires. We have made some initial research on the properties of the icosahedral nanowires reported in this paper. In particular we have examined their properties as surface-enhanced Raman spectroscopy (SERS) substrates. Metallic substrates play a fundamental role in detecting very low concentrations of molecules.[33] Recently Gunawidjaja *et al.*[34] have shown that gold nanowires mixed with silver nanoparticles are a very efficient substrate. According to those authors, the Raman intensity of the best-performing silver–gold nanostructure is comparable with the dense array of silver nanowires and silver nanoplates that were prepared by means of the Langmuir–Blodgett technique. An optimized design of a single-nanostructure substrate for SERS, based on a wet-assembly technique proposed here, can serve as a compact and low-cost alternative to fabricated nanoparticle arrays. However, by looking at the micrographs of the samples in ref 34 it is clear that the sample might be very inhomogeneous and not very reproducible. We have found that icosahedral bimetallic nanowires are extremely efficient SERS substrates. We have performed measurements using the standard rhodamine 6G (Rh6G) by Raman spectroscopy. The peak assignment of Rh6G adsorbed on colloidal silver is clearly identified: 614 cm^{-1} (C–C–C ring in-plane bending); 774 cm^{-1} (C–H in-plane bending); 1129 cm^{-1} (C–H in-plane bending), and 1183, 1310, 1363, 1509, and 1572 cm^{-1} (aromatic C–C stretching) among others. We observe a significant amplification of the peaks using icosahedral silver–gold nanowires. The intensity increases when the direction of the polarization of the laser beam is perpendicular to the edge of the nanowires (as expected for an elongated structure). However, because of the very small size of our nanowires, it is not possible to align all of them in the proper direction. In any case we estimate an amplification factor of 10^8–10^9. A typical SERS spectrum is shown in the Supporting Information.

Regarding electrical properties, we note the work of Hong *et al.*,[20] who obtained fcc bimetallic nanowires and demonstrated that they have remarkable Coulomb blockade effects. A similar property should be expected for 5-fold nanowires. We can visualize the technical feasibility of fabricating devices based on the packing of icosahedra and decahedra since the nanowires produced are in a solution and can be manipulated very easily.

CONCLUSIONS

We have shown that using an organometallic mixture it is possible to synthesize nanowires that show

true icosahedral and decahedral packing. Just as in the case of bulk quasicrystals, the introduction of a second atomic species was necessary to induce the 5-fold packing at the nanoscale level. In the present case the composition Ag/Au 3:1 favors this type of packing. However recent theoretical work[31] suggests that other concentrations should have similar effects and that other concentrations of the metals should produce new structures. Due to the stability of the icosahedra and decahedra nanowires with a composition Ag/Au 3:1, we can suggest the technical feasibility to fabricating devices based on these structures.

METHODS

Synthesis. Au nanowires were synthesized as follows: 6.6 mM $HAuCl_4 \cdot 3H_2O$ and 6.6 mM $AgNO_3$ were dissolved together in 10 mL of oleylamine ($C_{18}H_{37}N$) by vortex mixing at room temperature until the color of the solution changed from pale yellow to an intense orange color. This indicated the formation of a complex between Au^{3+} and OA. Then the solution was heated to 100 °C using an oil bath for 3 h. During this process the color of the solution changed from orange to pale yellow, indicating the reduction of Au^{3+} to Au^{+}. The color of the final solution that was obtained was red. This solution was dispersed in ethanol to obtain a black precipitate. This precipitate was separated from the solution by centrifugation (3000 rpm) for 15 min, cleaned several times with ethanol, and redispersed in 2 mL of hexane or chloroform for further analysis.

Electron Microscopy. For the electron microscopy analysis, a drop of the suspension was deposited onto a holey carbon grid. The samples were characterized using a JEOL JEM-2010F (FEG-TEM) operated at 200 kV with a 0.1 nm lattice resolution, which was employed to record high-resolution (HRTEM) images and electron diffraction (ED) patterns of the materials. For the aberration (Cs)-corrected characterization, the samples were analyzed using STEM with a JEOL ARM200F (200 kV) FEG-STEM/TEM, equipped with a CEOS Cs corrector on the illumination system. The probe size used for acquiring the HAADF as well as the Bright Field (BF)-STEM images was 9C (23.2 pA), and the CL aperture size was 40 μm. HAADF STEM images were acquired with a camera length of 8 cm/6 cm, and a collection angle of 68−280 mrad/90−270 mrad was used. The BF-STEM images were obtained using a 3 mm/1 mm aperture, and a collection angle of 17 mrad/5.6 mrad was used (camera length in this case was 8 cm). The HAADF as well as the BF images were acquired using a DigiScan camera. In order to reduce the noise of the images and to obtain clearer images, the raw data were filtered using the 2D Wiener filter and the Richardson−Lucy/maximum entropy algorithm implemented by Ishizuka.[35] The EDS analysis was performed using EDAX instrumentation attached to the JEOL ARM200F microscope. Spectra, line scans, and chemical maps for the various elements were obtained using the EDAX Genesis software. For the EDS analysis the probe size used was 0.8 nm and the condenser lens aperture size was 40 μm.

STEM and Molecular Dynamics Simulations. The STEM simulations were performed using the xHREM suite, which is based on the variant of Ishizuka of the FFT multislice method.[36] In accordance with the experimental setup, the simulated electron beam was 200 kV, with a resolution close to 0.1 nm and a defocus of 10 nm. The molecular dynamics simulations were made using the DL_POLY 2.14 code, by Smith and Forester.[37] The canonical ensemble runs were made using a Nose−Hoover thermostat with an inertial parameter of 0.1 and a time step of 0.0015 fs. The Sutton−Chen potential was parametrized following the work of Kimura,[38] with the usual rules for the definition of the alloy terms.

Acknowledgment. The authors would like to acknowledge The Welch Foundation Project AX-1615, "Controlling the Shape and Particles Using Wet Chemistry Methods and Its Application to Synthesis of Hollow Bimetallic Nanostructures". The authors would also like to acknowledge the NSF PREM Grant DMR 0934218, Title: Oxide and Metal Nanoparticles−The Interface between Life Sciences and Physical Sciences. The authors would also like to acknowledge RCMI Center for Interdisciplinary Health Research CIHR. The project described was supported by Award Number 2G12RR013646-11 from the National Center for Research Resources. The content is solely the responsibility of the authors and does not necessarily represent the official views of the National Center for Research Resources of the National Institutes of Health.

Supporting Information Available: This material is available free of charge *via* the Internet at http://pubs.acs.org.

REFERENCES AND NOTES

1. Torquato, S.; Stilinger, F. H. Jammed Hard-Particle Packings: From Kepler to Bernal and Beyond. *Rev. Mod. Phys.* **2010**, *82*, 2633–2672.
2. Boerdijk, A. H. Some Remarks Concerning Close Packing of Equal Spheres. *Philips Res. Rep.* **1952**, *7*, 303–313.
3. Coxeter, H. S. M. *Regular Complex Polytopes*; Cambridge University Press, 1st ed. 1974, 2nd ed. 1991.
4. Sedoc, J. F.; Rivier, N. Boerdijk−Coxeter Helix and Biological Helices as Quasicrystals. *Mat. Sci. Eng.* **2000**, *294−296*, 397–400.
5. Lord, E. A.; Ranganatan, S. The γ-Brass Structure and the Boerdijk−Coxeter Helix. *J. Non-Cryst. Solids* **2004**, *334−335*, 121–125.
6. Bernal, J. D. Geometry and the Structure of Monatomic Liquids. *Nature (London)* **1960**, *185*, 68–70.
7. Torquato, S.; Jiao, Y. Exact Constructions of a Family of Dense Periodic Packings of Tetrahedra. *Phys. Rev. E* **2010**, *81*, 041310.
8. Torquato, S.; Jiao, Y. Dense Packings of the Platonic and Archimedean Solids. *Nature* **2009**, *460*, 876–881.
9. Haji-Akbari, A.; Engel, M.; Keys, A.; Zheng, X.; Petschek, R.; Palffy-Muhoray, P.; Glotzer, S. C. Disordered, Quasicrystalline, and Crystalline Phases of Densely Packed Tetrahedra. *Nature* **2009**, *462*, 773–777.
10. Bilalbegovic, G. Assemblies of Gold Icosahedra. *Comput. Mater. Sci.* **2004**, *31*, 181–186.
11. Kondo, Y.; Takayanagi, K. Synthesis and Characterization of Helical Multi-Shell Gold Nanowires. *Science* **2000**, *289*, 606–608.
12. Bilalbegovic, G. Structure and Stability of Finite Gold Nanowires. *Phys. Rev. B* **1998**, *58*, 15412–15415.
13. Wang, B.; Yin, S.; Wang, G.; Buldum, A.; Zhao, J. Novel Structures and Properties of Gold Nanowires. *Phys. Rev. Lett. 86*, 2046−2049.
14. Halder, A.; Ravishankar, N. Ultrafine Single-Crystalline Gold Nanowire Arrays by Oriented Attachment. *Adv. Mater.* **2007**, *19*, 1854–1858.
15. Wang, C.; Hu, Y.; Lieber, C. M.; Sun, S. Ultrathin Au Nanowires and Their Transport Properties. *J. Am. Chem. Soc.* **2008**, *130*, 892002–8903.
16. Huo, Z.; Tsung, C.; Huang, W.; Zhang, X.; Yang, P. Sub-Two Nanometer Single Crystal Au Nanowires. *Nano Lett.* **2008**, *8*, 2041–2044.
17. Lu, X.; Yavuz, M. S.; Tuan, H.; Korgel, B.; Xia., Y. Ultrathin Gold Nanowires Can Be Obtained by Reducing Polymeric Strands of Oleylamine-AuCl Complexes Formed via Aurophilic Interaction. *J. Am. Chem. Soc.* **2008**, *130*, 8900.
18. Li, Z.; Tao, J.; Lu, X.; Zhu, Y.; Xia., Y. Facile Synthesis of Ultrathin Au Nanorods by Aging the AuCl (oleylamine) Complex with Amorphous Fe Nanoparticles in Chloroform. *Nano Lett.* **2008**, *8*, 3052–3055.

19. Krichevski, O.; Tirosh, E.; Markovich, G. Formation of Gold-Silver Nanowires in Thin Surfactant Solution Films. *Langmuir* **2006**, *22*, 867–870.
20. Hong, X.; Wang, D.; Yu, R.; Yan, H.; Sun, Y.; He, L.; Niu, Z.; Peng, Q.; Li, Y. Ultrathin Au−Ag Bimetallic Nanowires with Coulomb Blockade Effects. *Chem. Commun.* **2011**, *47*, 5160–5162.
21. Marks L. D. Particle Size Effects on Wulff Constructions. *Surf. Sci.* **1985**, *150* (2), 358−366
22. Ascencio, J. A.; Gutiérrez-Wing, C.; Espinosa, M. E.; Marín, M.; Tehuacanero, S.; Zorrilla, C.; José-Yacamán, M. Structure Determination of Small Particles by HREM Imaging: Theory and Experiment. *Surf. Sci.* **1998**, *396*, 349–368.
23. Varela, M.; Lupini, A. R.; Van Benthem, K.; Borisevich, A. Y.; Chisholm, M. F.; Shibata, N.; Abe, E.; Pennycook, S. J. Materials Characterization in the Aberration-Corrected Scanning Transmission Electron Microscope. *Annu. Rev. Mater. Res.* **2005**, *35*, 539–569.
24. Legoas, S. B.; Galvão, D. S.; Rodrigues, V.; Ugarte, D. Origin of Anomalously Long Interatomic Distances in Suspended Gold Chains. *Phys. Rev. Lett.* **2002**, *88*, 076105.
25. Coura, P. Z.; Legoas, S. B.; Moreira, A. S.; Sato, F; Rodrigues, V.; Dantas, S. O.; Ugarte, D.; Galvão., D. S. On the Structural and Stability Features of Linear Atomic Suspended Chains Formed from Gold Nanowires Stretching. *Nano Lett.* **2004**, *4*, 1187–1191.
26. González, J. C.; Rodrigues, V.; Bettini, J.; Rego, L. G. C.; Rocha, A. R.; Coura, P. Z.; Dantas, S. O.; Sato, F.; Galvão, D. S.; Ugarte, D. Indication of Unusual Pentagonal Structures in Atomic-Size Cu Nanowires. *Phys. Rev. Lett.* **2004**, *93*, 126103 1–4.
27. Sánchez-Portal, D .; Artacho, E.; Junquera, J.; Ordejón, P.; Garca, A.; Soler, J. M. Stiff Monatomic Gold Wires with a Spinning Zigzag. *Geometry* **1999**, *83*, 3884–3887.
28. Park, H. S.; Zimmerman, J. A. Modeling Inelasticity and Failure in Gold Nanowires. *Phys. Rev. B* **2005**, *72*, 054106.
29. Marks, L. D. Modified Wulff Constructions for Twinned Particles. *J. Cryst. Growth* **1983**, *61*, 556–566.
30. Kroner, E.; Anthony, K. H. Dislocations and Disclinations in Material Structures: The Basic Topological Concepts. *Annu. Rev. Mater. Sci.* **1975**, *5*, 43–72.
31. Cerbelaud, M.; Ferrando, R.; Barcaro, G.; Fortunelli, A. Optimization of Chemical Ordering in AgAu Nanoalloys. *Phys. Chem. Chem. Phys.* **2011**, *13*, 10232–10240.
32. Louzguine-Luzgin, D. V.; Inoue, A. Formation and Properties of Quasicrystals. *Ann Rev. Mater. Res.* **2008**, *38*, 403–423.
33. Fan, M.; Andrade, G.; Brolo, A. G. A Review on the Fabrication of Substrates for Surface Enhanced Raman Spectroscopy and Their Applications in Analytical Chemistry. *Anal. Chim. Acta* **2011**, *693*, 7–25.
34. Gunawidjaja, Ray.; Kharlampieva, E.; Choi, I.; Tsukruk, V. V. Bimetallic Nanostructures as Active Raman Markers: Gold-Nanoparticle Assembly on 1D and 2D Silver Nanostructure Surfaces. *Small* **2009**, *5*, 2460–2466.
35. Ishizuka, K. A Practical Approach for STEM Image Simulation Based on the FFT Multislice Method. *Ultramicroscopy* **2001**, *90*, 71–83.
36. HREM Research Inc., http://www.hremresearch.com.
37. Forester, T. R.; Smith, W. DL_POLY Molecular Dynamics Code, CCP5, **1995**.
38. Kimura, Y. Technical Report 3, Caltech ASCI, **1998**.